Computational Design Methods Comparison for the Optimization of Variable Section Continuous Beams

Computational design methods comparison for the optimization of variable section continuous beams

Laura Sardone
Department of Structural, Geotechnical and Building Engineering
Politecnico di Torino
Turin, Italy
ORCID ID: 0000-0002-0928-0606

Stefanos Sotiropoulos
Department of Computer Science
University of Bari "Aldo Moro"
Bari, Italy
ORCID ID: 0000-0001-5669-1320

***Abstract*—In recent years, novel computational tools such as generative or parametric design revolutionized the existing approaches to architecture and engineering, substantially affecting and also improving the structural optimization field. This latter can be formally conceived as three different sub-problems, thus involving size optimization, shape optimization, and topology optimization. In this study, the authors mainly focused on solving joint size and shape optimization problems for a continuous variable section simply supported beam domain by comparing the optimization precision obtained among two different computational design methodologies. The former method relies on visual programming parametric design based on Grasshopper software, whilst the second approach is based on the analytical resolution of the multi-domain beam's differential equations directly implemented in the MATLAB software. The currently considered test case geometry is based on the iconic continuous beam geometry designed by P. M. da Rocha and the engineer S. Mitsutani built for the Japan World Exposition, Osaka, 1970 (Osaka's Expo '70), but today no longer exists since already dismantled and demolished. This was a reference benchmark in the architectural field characterized by an optimized shape with circular soffit geometry at constant curvature. The results of the study show, in the search for the architectural optimal solutions, advantages regarding the performance of the structures and the control of the shape of the architectural component giving, at the same time, the possibility to join the needs of architectural narratives with the stability and efficiency of an optimized and correctly designed structure.**

Keywords— Generative Design, Visual Programming, Computational Geometry, Design Optimization, Structural Optimization, Conceptual Design.

I. INTRODUCTION

In civil engineering and the architecture fields, the need for shape control and the boom of design creativity thanks to the wide use of new modeling tools, lead to different structural solutions and expressions, giving the structural-design world new challenges. One of the most common structural elements used to aim for specific shapes and simultaneously join geometric/architectural needs with the structural design and the shape optimization is the case of the beams with non-constant (or variable) cross-sections. These elements represent a class of slender bodies, the aim of practitioners' interest due to the possibility of the adoption of different geometry considering different needs.

The multitude of advantages given by free-form beams is however accompanied by different problems that take place with the non-prismatic beam modeling which often leads to inaccurate predictions that vanish the gain of the optimization process. Therefore, an effective non-prismatic beam modeling still represents a branch of the structural engineering of interest for the community, especially for advanced design applications in large spans elements [1]. The reversibility that the variable-section beams have towards architecture has meant that these elements are more frequently combined with the concept of large spans. This latter theme leads often to the search of the best solution considering that as the span of a structure increases, the structural performance will have to increase at the same rate since the self-weight can become excessive, significantly affecting deformations, and amplifying seismic action, so requiring suitable design strategies able to reduce volume [2].

Joining parameters like large span and non-constant cross-section in a beam means questioning different disciplines and evaluating them as design variables in all phases of the entire process, from the first phase called "conceptual design" to the final phase construction step. In this contribution, we aim to present a design process that can consider shape research as a geometrical decision (or constraint) to achieve a design method to assign shape obtaining performative structure elements.

Nowadays, the optimization techniques available are endless, however, two numerical methodologies will be explored in this paper through the use of formulations based on computational geometry in which, in this field become a necessity to control the shape of structural elements. In particular, the adopted solvers in the two methodologies developed are i) MATLAB-GA, a stochastic, population-based algorithm that randomly searches the optimal solution among population members, by mutation and crossover operators; ii) Gh-Octopus, a Multi-Objective Evolutionary Optimization solver, which allows the production of optimized trade-off solutions between the extremes of each goal, able to support designers in decision making.

A. Merging computational design with architectural needs: the case study

Recognizing architectural design as an extremely complex and multifaceted discipline has allowed the drafting of this document, within which there is the effort of combining morphological parameters with structural design. This effort ended with the implementation of a design methodologies assisted by algorithms merged with geometrically constrained structural optimization using evolutionary genetic algorithms.

Among the most significant examples of structures characterized by large spans in which a continuous beam with variable cross-section is adopted, we find a specific admirable case in the architectural production of the architect Paulo Mendes da Rocha with his project for the Japan World Exposition, Osaka, 1970 (Osaka's Expo '70) (Figure 1).

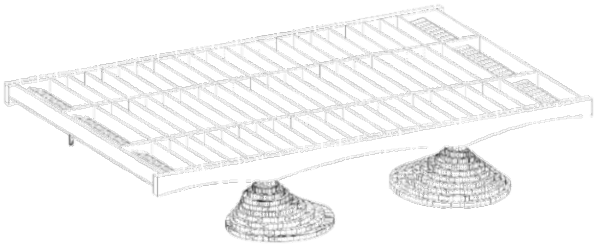

Fig. 1. Brazilian Pavilion, Japan World Exposition, Osaka, 1970

The structure is composed of a platform of 1,500 square meters casts shade on the terrain that undulates until touching the roof at three different points, with no transition supports. Two main longitudinal beams with variable depth with the two crossbeams generate a rectangular section of 32.5m*50.00m orthogonal grid closed horizontally with a pyramid-shaped coffering and glass panels [3]. The architectural function is completely transferred on the shape of the structure, made of concrete and steel [4] [5] [6].

In this contribution, the focus is on the main beams with a non-constant section (Figure 2) starting - to conduct a correct analysis - from the redesign of the structural element.

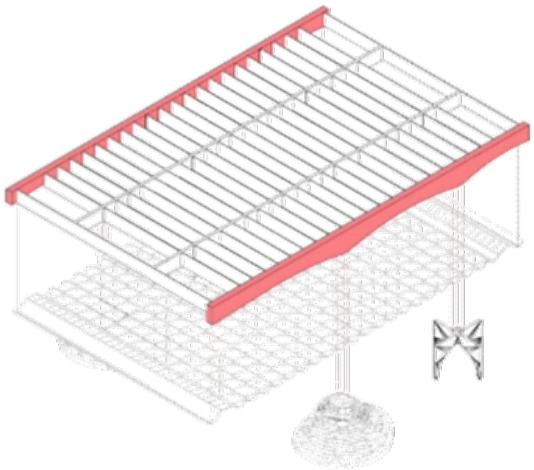

Fig. 2. Exploded view of the Brazilian Pavilion at the Osaka Expo, 1970. In red: main beams with variable cross-section.

In the next sections of this contribution, the implementations of the methodologies suitable for the development of the analysis and optimization will be shown out by imposing geometric constraints. The advantage of the developed methodologies is given by the reversibility of the produced codes which allows the user to be able to work on multiple structural shapes and different elements.

II. COMPUTATIONAL GEOMETRY AND ANALYTICAL MODEL OF THE VARIABLE SECTION BEAM

Starting from the parameterization of the variable-section beam of the case study, parameters such as the total length, the internal spans, the height, and thickness were set as constant, setting three different reference axes to facilitate the computational development of the shape of the structural object. The parameters are described in Table 1.

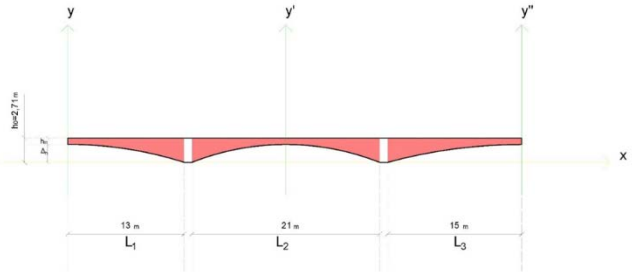

Fig. 3. Geometry of the main beam with non-constant section and reference axes

TABLE I. PARAMETER'S SELECTION OF THE VARIABLE-SECTION BEAM.

h0 [m]	**b0 [m]**	**L1, L2, L3 [m]**	**Length (distribution) support points [m]**	**hm [1,2,3]**
2.71	0.9	[13; 21; 15]	0.9	h0-*$\Delta h_{[1,2,3]}$
With *$\Delta h_{[1,2,3]} \in$ [0, +2.71] (m) ($\cap$ y axis)				

The shape is described by the set of the physical parameters as follows:

$$\{p_i\}_{i=1,\cdots,N} \quad (1)$$

in which we will define the parameters describing the only optimization variable.

The arc of circumference in our case represents the geometric constraint to be imposed in the optimization phase (Section 3), therefore, considering the general equation of the circumference in XY-plane as follows:

$$x^2 + y^2 + ax + by + c = 0 \quad (2)$$

where a, b and c are real coefficients.

Considering the single span (Figure 4), the beam domain can be assumed as a rectangle in the bi-dimensional XY-plane characterized by span length L and full cross section depth h_0 and with constant width b_0.

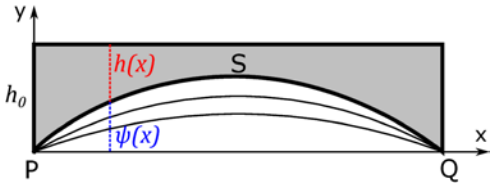

Fig. 4. XY-plane characterized by span length L and full cross section depth h_0 and with constant width b_0.

To optimize the beam shape and at the same time the volume of the structural element, the solver is supposed to move the inner surface i.e., the lower beam profile following a curved shape defined by a certain emptying function, in this case, given by ψ(x) retrieved considering the Equation (2).

The adoption of a circular arc emptying profile led to some benefits, one of them is the fact that this kind of profile is characterized by a constant curvature. From the constructive point of view, it is thus easier to realize a formwork with a constant curvature with respect to another profile with a variable curvature which requires special techniques e.g., with special fabric formwork [7]. The emptying function ψ(x) is formalized considering a circumference passing through three arbitrary points P, Q and S, which coordinates are given as follows:

$$P = (x_p = 0; y_p = 0), \quad (3)$$

$$Q = (x_Q = 0; y_Q = 0), \quad (4)$$

$$S = \left(x_s = \frac{x_P + x_Q}{2}; y_s = \Delta h\right) \quad (5)$$

in which the emptying magnitude Δ_h is governed by the y-coordinates of the point S. In general, the circumference equation is given by Equation (2) from which it is possible to find the center point *C* as

$$C = (x_C; y_C) = \left(-\frac{a}{2}; -\frac{b}{2}\right) \quad (6)$$

and the radius of curvature as

$$R = \frac{1}{2}\sqrt{a^2 + b^2 - 4c} \quad (7)$$

The parameters *α, b,* and *c* in Equation (2) are governing the position and the shape of the circumference in the XY-plane. To define their value, it is sufficient to impose the coordinates of the points P, Q ed S defined in Eqs. (3) (4) (5) in Equation (2) thus solving the following linear system of three equation with three unknowns:

$$\begin{cases} x_p^2 + y_p^2 + a_{xp} + b_{yp} + c = 0 \\ x_Q^2 + y_Q^2 + a_{xQ} + b_{yQ} + c = 0 \\ x_S^2 + y_S^2 + a_{xS} + b_{yS} + c = 0 \end{cases} \quad (8)$$

which can be rewritten in matrix form such as

$$\begin{bmatrix} x_p & y_p & 1 \\ x_Q & y_Q & 1 \\ x_s & y_s & 1 \end{bmatrix} \begin{bmatrix} a \\ b \\ c \end{bmatrix} = \begin{bmatrix} -x_P^2 & -y_P^2 \\ -x_Q^2 & -y_Q^2 \\ -x_S^2 & -y_S^2 \end{bmatrix} \quad (9)$$

Once the circumference equation has been determined for the coordinates of the points *P*, *Q* and *S*, it is possible to get the effective beam depth as the difference between the constant function of the initial depth of the beam h0 and the emptying function:

$$h(x) = h_0 - \psi(x) \quad (10)$$

in which ψ (x) =y(x) i.e. the emptying function follows the circumference in Equation (2) for all $x \in [x_P, x_Q]$. Therefore, considering a certain abscissa X, it is possible to rewrite the Equation (2) to solve it concerning the position of the Y-axis and considering the right-hand side (RHS) member of the following equation as a constant term denoted as $d(x) = x^2 + |a|x$:

$$y^2 + by = -x^2 + |a|x \Rightarrow y^2 + b_y = -d \quad (11)$$

It is now possible to solve Eq. (11) using the Quadratic Formulae for quadratic equations, noticing that it is necessary to retain the positive sign of the root square term which is referred to the upper part of the circumference, obtaining the analytical relationship of ψ (x):

$$\psi(x) = y(x) = \frac{-b + \sqrt{b^2 - 4d}}{2} \quad (12)$$

To consider possible variable cross-section cantilever geometries, the overall process is reiterated observing that in our implementation for a left cantilever, the point P has to be located with coordinates that are symmetrical considering the y-axis to the coordinates of Q in a way that the point S is located to the tip of the cantilever. Vice versa, for a right cantilever, the point Q must be located with coordinates that are double of the P coordinates, which always leads to situate the point S at the tip of the cantilever. As shown in Figure 3, the present case study is referred to a multi-domain beam which is characterized by a simply supported beam with two cantilevers, one on both sides of the beam. Therefore, as illustrated in Figure 5, for this problem it is possible to consider three sub-domains or sub-regions, each of them characterized by a local reference system $(x_i O_i y_i)$ with as the first region (i) the left cantilever (L_1= 13.45m), as a second region (ii) the simply supported region (mid-section, L_2=21.90 m) and as a third region (iii) the right cantilever (L_3=15.45 m).

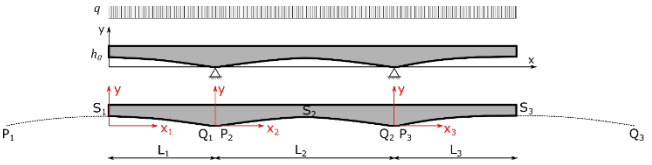

Fig. 5. Multi-domain subdivision related to the case study problem.

The equation of elastic line of the variable section beam [8] can be written as:

$$\frac{d^2}{dx^2}\left[EJ(x)\frac{d^2}{dx^2}y(x)\right] = q(x) \quad (13)$$

where x is the longitudinal coordinate of the beam axis, y is the beam deflection, E is the elastic modulus, J(x) represents the moment of inertia variable along the x coordinate and q(x) is the distributed load which comprises both self-weight and live load applied on the non-prismatic beam element. Considering (13), the necessary condition is to take into account the first and second derivative of the inertia moment, which is directly dependent on the variable depth of the section of the beam:

$$h'(x) = -\psi'(y) \quad (14)$$

$$h''(x) = -\psi''(y) \quad (14.1)$$

Considering the analytical model of the beam we obtain a system of a fourth order equations:

$$\begin{cases} y_1^{IV}(x_1) + y_1^{III} \cdot A_1 + y_1^{II} \cdot A_2^I + A_3^I = 0 \\ y_2^{IV}(x_1) + y_2^{III} \cdot A_1^{II} + y_2^{II} \cdot A_2^{II} + A_3^{II} = 0 \\ y_3^{IV}(x_1) + y_3^{III} \cdot A_1^{III} + y_3^{II} \cdot A_2^{III} + A_3^{III} = 0 \end{cases} \quad (15)$$

in which we are considering the inertia moments and its derivative. Overlapping the derivative of the inertia moment with the derivative of (14) and (14.1) we retrieve:

$$J(x) = \frac{1}{12} b[h_0 - \psi]^3 \quad (16)$$

$$J'(x) = \frac{1}{4} b[h_0 - \psi]^2(-\psi') \quad (16.1)$$

$$J''(x) = \frac{1}{4} b[2(h_0 - \psi)(-\psi')^2 + (h_0 - \psi)^2(-\psi'')] \quad (16.2)$$

where:

$$\psi' = \frac{-d'}{\sqrt{b^2 - 4d}} \quad (16.2.1)$$

$$\psi'' = \frac{-d''(b^2 - 4d) - 2(d')^2}{(b^2 - 4d)^{\frac{3}{2}}} \quad (16.2.2)$$

represents the derivatives of the emptying function introduced in (10).

A. *The Optimization Problem*

Considering the set of physical parameters described in (1), the optimization problem can be written as follow:

$$\min_{\{p_i\} \in P_{ad}} V_1 \tag{17}$$

where in (1) are included, the parameters described as $\Delta_{h\,[1,2,3]}$ in Table 1 and V_1 is representing the total volume to be minimized. The Objective Function will be subjected to

$$g_1 = g_3 \leq \frac{1}{250} L_{1,3} \tag{17.1}$$

$$g_2 \leq \frac{1}{150} L_2 \tag{17.2}$$

In which g_1, g_2, and g_3 are describing the maximum displacement allowed at the mid-span (L_2, g_2) and at the external point of the cantilevers beam (g_1, g_3). Furthermore, the evaluation of the mass of the beam subject to the emptying function can be considered as a beam with a solid geometry to which the area subtended by the curve of the arc of the circumference must be subtracted. Knowing that the area of the circular segment is equal to the difference between the area of the circular sector and that of the isosceles triangle, being Θ the angle at the center that subtends the arc of the circumference and knowing the coordinates of the center of the circumferences we can obtain Θ with:

$$\theta = 2 \arccos \frac{|y_c|}{R} \tag{18}$$

showing that the area of the circular segment is equal to

$$A = \frac{1}{2} R^2 (\theta - \sin(\theta)) \tag{19}$$

and that the volume of the beam subjected to the emptying function is equal to

$$O.F. = V = b_0 [h_0 \cdot L - A] \tag{20}$$

obtaining the Objective Function of the problem related to the beam with a non-constant cross-section subjected to the circular emptying function.

III. Numerical Development through Visual Programming Language

Starting from the geometric model, to obtain the solution of the optimization problem it was necessary to specify the material and the cross-section dimensions. The numerical development, for this first stage, has been carried out using Visual Programming Language (VPL) (Grasshopper in Rhinoceros 3D). Using Karamba 3D Plug-in, it is possible to retrieve a shell model from given meshes as input and define at the same time the cross-section of the shell element. In this case, the cross-section is given by "Shell Constant" which allows the setting of the height and material of a shell with a constant cross-section; the material selected belongs to the concrete family with a compression strength of 45 MPa (C45/55).

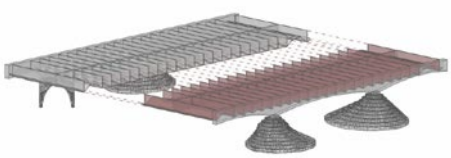

Fig. 6. Portion of the roof considered for the load implementation.

The load imposed in the numerical model – additionally to the self-weight - has been extrapolated directly from the volume of the case study as follow:

$$\gamma C45 \,/\, 55 \cdot \frac{Volume}{2} \tag{21}$$

$$25kN/m^3 \cdot \frac{369}{z} m^3 = 4612.5kN \tag{21.1}$$

$$\frac{4612.5}{L} kN = 90.44kN/m \tag{21.2}$$

For a continuous beam simply-supported in two discontinuous regions, the boundary conditions are:

TABLE II. Boundary conditions applied.

Boundary conditions	**0**	**1**	**1'**	**2'**	**2**	**3**
T	0	ql_1	$\frac{ql}{2} - \frac{M_2 - M_1}{l}$	$\frac{ql}{2} + \frac{M_2 - M_1}{l}$	ql_2	0
N	0	0	0	0	0	0
M	0	$\frac{ql_1^2}{2}$	$\frac{ql_1^2}{2}$	$\frac{ql_2^2}{2}$	$\frac{ql_2^2}{2}$	0
ρ	$\frac{Ml_1^2}{2EJ}$	ρ1=ρ1'	ρ1=ρ1'	ρ2=ρ2'	ρ2=ρ2'	$\frac{Ml_2^2}{2EJ}$
δ_{max}	$\frac{Ml_1}{EJ}$	0	0	0	0	$+\frac{Ml_2}{EJ}$

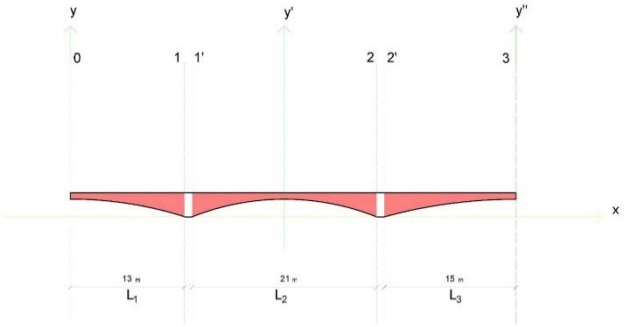

Fig. 7. Application of boundary conditions; sections related to the Table 2.

The shape variation depending on the parameters included in (17) will allow a possible set of solutions included in the Pareto-Optimal front. The solver in the optimization process will find the best shape of the structural element to allow the volume to be optimized but at the same time to minimize the displacement represented in (17.1) and (17.2).

In the entire process, different plug-in are involved: i) grasshopper, adopted for the parametric model; ii) Karamba 3D used to obtain the output for FEA Results; Octopus plug-in (MOOPs) adopted as an optimization solver. In the proposed optimization problem, the only parameter considered as a variable design vector is the amplitude $\Delta_{h[1,2,3]}$ (Figure 3), while the displacement δ will represent the constraints called - in this process - *Boolean Hard Constraints* where the optional boolean parameters can be connected. Octopus expects a "true" value for every valid solution, otherwise, the solution is discarded; in this way, the constraint is becoming - at the same time - part of the objective function allowing us to rewrite (17) in the following way for the specific condition:

$$\min_{\{p_i\} \in P_{ad}} V_1, \delta_n \tag{17.3}$$

subjected to

$$\delta_1 = \delta_3 \leq \frac{1}{250} L_{1,3} \tag{17.3.1}$$

$$\delta_2 \leq \frac{1}{150} L_2 \tag{17.3.2}$$

In which δ_1 represent the maximum displacement detectable in the whole beam element minimized in the optimization process.

IV. Numerical Development and Optimization Comparison with Matlab implementation

To validate the VPL code, a MATLAB script was also implemented. The structural analysis has been performed by adopting the Timoshenko-like beam model, a simplified model for variable cross section [9],[10],[11] which adopts a system of six ordinary differential equations (ODEs):

$$\begin{Bmatrix} u'(x) \\ v'(x) \\ \phi'(x) \\ M'(x) \\ V'(x) \\ N'(x) \end{Bmatrix} = \begin{bmatrix} \varepsilon_H & \varepsilon_V & \varepsilon_M & -c(x) & 0 & 0 \\ \gamma_H & \gamma_V & \gamma_M & 1 & 0 & 0 \\ x_H & x_V & x_M & 0 & 0 & 0 \\ c(x) & -1 & 0 & 0 & 0 & 0 \\ 0 & 0 & 0 & 0 & 0 & 0 \\ 0 & 0 & 0 & 0 & 0 & 0 \end{bmatrix} \begin{Bmatrix} u(x) \\ v(x) \\ \phi(x) \\ M(x) \\ V(x) \\ N(x) \end{Bmatrix} - \begin{Bmatrix} 0 \\ 0 \\ 0 \\ m(x) \\ q(x) \\ p(x) \end{Bmatrix} \tag{22}$$

In which

$$\varepsilon_H(x) = \left(\frac{c'^2(x)}{5Gh(x)} + \frac{h'^2(x)}{12Gh(x)} + \frac{1}{Eh(x)} \right) \tag{22.1}$$

$$\varepsilon_M(x) = X_H(x) = \frac{8c'(x)h\prime(x)}{5\,\mathrm{Gh}^2(x)} \tag{22.2}$$

$$\varepsilon_V(x) = \gamma_H(x) = \frac{c'(x)}{5\,\mathrm{Gh}^2(x)} \tag{22.3}$$

$$X_M(x) = \left(\frac{9h'^2(x)}{5Gh^3(x)} + \frac{12c'^2(x)}{Gh^3(x)} + \frac{12}{Eh^3(x)} \right) \tag{22.4}$$

$$X_V(x) = \gamma_M(x) = \frac{3h'(x)}{5\,\mathrm{Gh}^2(x)} \tag{22.5}$$

$$\gamma_H(x) = \frac{6}{5\,Gh(x)} \tag{22.6}$$

In the previous equations the terms N(x), V(x) and M(x) represent the axial force internal action, the bending moment, and the shear each section in any position x respectively, while the terms u(x), υ(x)and ϕ(x) represent the horizontal displacement, the vertical displacement, and the rotation of each cross section respectively. The terms m(x), q(x) and p(x) are related to distributed moments, distributed vertical loads, and distributed axial loads applied along the beam, respectively. The process to obtain the above formulations is well defined in [9],[10],[11]. In the constitutive terms, the G represents the tangential modulus of the material, E denoted the elastic modulus. The term c(x) represents the equation of the center line of the variable cross section beam. Finally, the quote mark in the previous terms represent the first derivative respect to the x abscissa ($\frac{d}{dx}$).

The analytical model presented above has been adapted for the case study, considering three sub-regions in which solve the system of six ODEs. This system has been numerically solved with Matlab solver *bvp4c* adopting the multi-domain approach which required eighteen boundary condition (BCs). The BCs are defined looking to statics, kinematics, restraints, external conditions, and continuity conditions among the domains. Since this specific analytical model tries to be more complete than the elastic line presented in (13), it now requires 6 BCs for each domain considering also the axial conditions. Considering two fixed supports as external restraints and posing all the continuity conditions in the touching boundaries between two consequently domains, in the Table 2 the BCs for the Matlab implementation are presented.

TABLE III. Boundary conditions applied in Matlab. Section positions are the same depicted in Figure 7

Boundary conditions	0	1	1'	2'	2	3
T	0					0
N	0					0
M	0	$M_1 = M_{1'}$		$M_2 = M_{2'}$		0
v		0	0	0	0	
u		0	0	0	0	
ϕ		$\phi_1 = \phi_{1'}$		$\phi_2 = \phi_{2'}$		

In the GA Matlab implementation stress constraints are also accounted adopting the simplified Von Mises stress verification for the most stressed points of each cross section under the hypothesis of homogenous material.

$$\sigma^2(x,y) + 3\tau^2(x,y) \leq \sigma^2_{id,VM}, \tag{23}$$

V. Numerical Results and Discussion

In the following sections the numerical results retrieved by the two methodologies applied are discussed.

A. Gh-Octopus Results

After 300 generations, with a population size equal to 20, the non-dominated solutions are shown in the following graph (Figure 7):

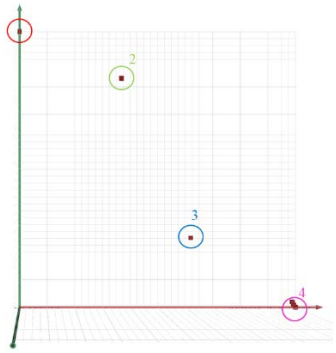

Fig. 8. Pareto-Optimal Front in Gh-Octopus

For a non-trivial multi-objective optimization problem, there is no single solution that simultaneously optimizes all objectives. In this case, the objective functions are said to be in conflict, and there is an infinite number of possible Pareto-optimal solutions. A solution is called non-dominated, Pareto optimal, or Pareto efficient, if none of the objective functions can improve its value without worsening the others. In this case, we can observe *four* of the *non - dominated* solutions in which no constraints have been violated (Table 4).

TABLE IV. Pareto – Optimal front solutions (Figure 9).

Solutions	Mass [Kg]	δ_{max} [cm]
S1	145321.89	4.9
S2	187840.82	4.3
S3	216893.00	4.88
S4	260720.59	4.4

The advantage, in this case, is to have feasible solutions having the possibility to choose between each of them, respecting the will of the designer also through the imposed geometries (Figure 8).

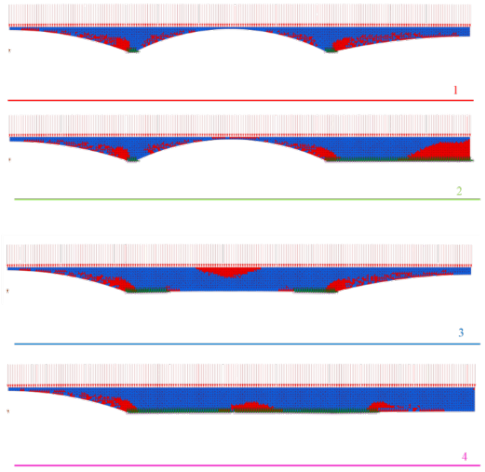

Fig. 9. Solution developed by Octopus Solver summarized in Table 3.

In the following image, a comparative draw has been developed to compare the shape of the main beam of the Brazilian pavilion in Osaka and the one optimized by the solver (Figure 9).

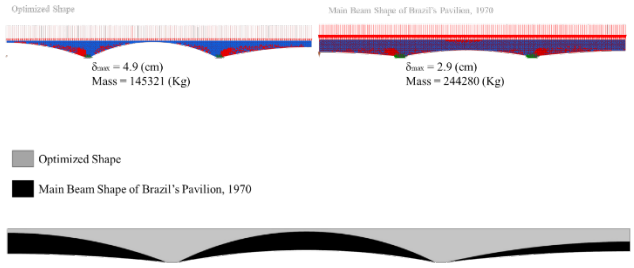

Fig. 10. Shape Comparison between the main beam of Brazil's Pavilion (Expo Osaka, 1970) and the beam subjected to the Optimization process.

B. *Matlab-GA results*

The following results (Figure 11) are retrieved considering 10 runs from the Matlab code developed considering the Balduzzi analysis applied and solved through GA, setting 20 generations and the population size equal to 10: optimal maximum emptying values Δ_h for the Region i, ii and iii with circular arc emptying function, maximum theoretical volume and optimal volume; the results are summarized in Table 5.

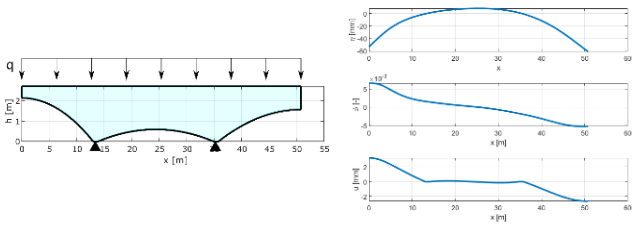

Fig. 11. Matlab-ga shape result and graphs

TABLE V. MATLAB-GA RESULTS.

Matlab-ga results	**Region (i)**	**Region (ii)**	**Region (iii)**
Δ_h [m]	2.14	0.60	1.57
O.F. Max [m^3]	123.9		
O.F. Opt. [m^3]	85.4		

C. *Results Discussion*

In this scientific contribution, a new methodology for a preliminary optimization of a structural element has been presented and tested using innovative tools joining the power of computational design with generative algorithms. Through the use of numerical methods, the time of evaluation and optimization has been reduced considering the complexity of calculation; moreover, through visual programming, it is possible to implement accurate analysis for the pre-processing and post-processing (FEM) of the element to be optimized without necessarily applying different programming techniques having in any case, the opportunity to integrate functions and codes external to the Grasshopper environment.

The two different methodologies applied to implement the numerical solution of the Optimization Problem, are showing different solutions due to the different implementation of the problem; despite the difference regarding the size of the variable cross-section beam, the results can be comparable considering the geometrical constraint applied (introduced (2)).

ACKNOWLEDGMENT

This study was carried out within the RETURN Extended Partnership and received funding from the European Union Next-GenerationEU (National Recovery and Resilience Plan – NRRP, Mission 4, Component 2, Investment 1.3 – D.D. 1243 2/8/2022, PE0000005).

REFERENCES

[1] V. De Biagi, B. Chiaia, G.C. Marano, A. Fiore, R. Greco, L. Sardone, R. Cucuzza, G.L. Cascella, M. Spinelli, N.D. Lagaros, Series solution of beams with variable cross-section. Jan. 2020, Procedia Manufacturing 44:489-496, DOI: 10.1016/j.promfg.2020.02.265.

[2] L. Sardone, R. Greco, A. Fiore, C. Moccia, D. De Tommasi, N. D. Lagaros. A prelimi-nary study on a variable section beam through Algorithm-Aided Design: A way to con-nect architectural shape and structural optimization. Procedia Manuf 2020;44: 497–504. https://doi.org/10.1016/j.promfg.2020.02.264.

[3] L. Fernandez-Galiano, AV, Arquitectura Viva SL, Monografías N°161, Paulo Mendes da Rocha, Brazilian Pavilion for Expo 70, Osaka, p.24, Madrid, May 2021.

[4] AR Editors, Brazilian pavilion, Osaka Expo, by Paulo Mendes da Rocha, in Architec-tural Review, 16 October 2019, available on line on www.architectural-review.com/buildings.

[5] R. V. Zein and I. Amaral, "Osaka World's Fair of 1970 and the Brazilian Pavilion", ArqTexto, 16 (2010), 108-127, p. 113.

[6] R. Selby, Brazilian Pavilion – 1970 Osaka World Fair, Understanding brutalism in Brazil through a short writing on a building case study, June 2016, Newcastle University. Available on https://brazilianconcrete.wordpress.com/2016/06/15/brazilian-pavilion-1970-osaka-world-fair/.

[7] D. Veenendaal. "Evolutionary Optimization of Fabric Formed Structural Elements". Master'sthesis, Technische Universiteit Delft, Netherlands, 2008.

[8] S. Timoshenko, 1951. Theory of elasticity, McGraw Hill, New York (3d Edition).

[9] G, Balduzzi, M. Aminbaghai, E. Sacco, J. Füssl, J. Eberhardsteiner, and F. Auricchio. "Non-prismatic beams: A simple and effective Timoshenko-like model". International Journal of Solids and Structures, 90:236–250, 2016.

[10] G. Balduzzi, S. Morganti, F. Auricchio, and A. Reali. "Non-prismatic Timoshenko-like beam model: Numerical solution via isogeometric collocation". Computers & Mathe-matics with Applications, 74(7):1531–1541, 2017. High-Order Finite Element and Iso-geometric Methods2016.

[11] G. Balduzzi, M. Aminbaghai, F. Auricchio, and J. Fssül. "Planar Timoshenko-like mod-el for multilayer non-prismatic beams". International Journal of Mechanics and Materials in Design, 14:51–70, 2018